Diagn Interv Radiol 2014; 20:90–99

PEDIATRIC RADIOLOGY
ORIGINAL ARTICLE

Measurement of real-time tissue elastography in a phantom model and comparison with transient elastography in pediatric patients with liver diseases

Jens-Peter Schenk, Gerhard Alzen, Volker Klingmüller, Ulrike Teufel, Saroa El Sakka, Guido Engelmann, Buket Selmi

PURPOSE
We aimed to determine the comparability of real-time tissue elastography (RTE) and transient elastography (TE) in pediatric patients with liver diseases.

MATERIALS AND METHODS
RTE was performed on the Elasticity QA Phantom Model 049 (Computerized Imaging Reference Systems Company Inc., Norfolk, Virginia, USA), which has five areas with different levels of stiffness. RTE measurements of relative stiffness (MEAN [mean value of tissue elasticity], AREA [% of blue color-coded stiffer tissue]) in the phantom were compared with the phantom stiffness specified in kPa (measurement unit of TE). RTE and TE were performed on 147 pediatric patients with various liver diseases. A total of 109 measurements were valid. The participants had following diseases: metabolic liver disease (n=25), cystic fibrosis (n=20), hepatopathy of unknown origin (n=11), autoimmune hepatitis (n=12), Wilson's disease (n=11), and various liver parenchyma alterations (n=30). Correlations between RTE and TE measurements in the patients were calculated. In addition, RTE was performed on a control group (n=30), and the RTE values between the patient and control groups were compared.

RESULTS
The RTE parameters showed good correlation in the phantom model with phantom stiffness (MEAN/kPa, r=-0.97; AREA/kPa, r=0.98). However, the correlation of RTE and TE was weak in the patient group (MEAN/kPa, r=-0.23; AREA/kPa, r=0.24). A significant difference was observed between the patient and control groups (MEAN, P = 5.32 e-7; AREA, P = 1.62 e-6).

CONCLUSION
In the phantom model, RTE was correlated with kPa, confirming the presumed comparability of the methods. However, there was no direct correlation between RTE and TE in patients with defined liver diseases under real clinical conditions.

From the Division of Pediatric Radiology (J-P.S., S.E.S., B.S. ✉ *buketselmi@gmail.com*), Department of Diagnostic and Interventional Radiology, University Hospital of Heidelberg, Heidelberg, Germany; the Department of Pediatric Radiology (G.A., V.K.), University Clinic Giessen & Marburg, Giessen, Germany; the Department of General Pediatrics (U.T., G.E.), University Hospital of Heidelberg, Germany.

Received 7 March 2013; revision requested 4 April 2013; revision received; 21 June 2013; accepted 22 June 2013.

Published online 4 December 2013.
DOI 10.5152/dir.2013.13116

Liver histology is considered a gold standard for detecting liver diseases. However, due to its various limitations, including pain, sampling variability and even death, many non-invasive methods have been developed as alternative approaches to liver biopsy (1–4). The ultrasonographic methods include transient elastography (TE; Fibroscan®, Echosens, Paris, France), real-time tissue elastography (RTE; Hitachi, Tokyo, Japan), acoustic radiation force impulse imaging (ARFI; Siemens Healthcare, Erlangen, Germany), and real-time shear wave elastography (SWE; SuperSonic Imagine S.A., Aix-en-Provence, France).

TE was the first ultrasonography (US) method for determining liver elasticity, and it was introduced in 2003 (5). Since 2008, with the introduction of a new, appropriate probe with a smaller diameter (S-probe), the method has also been used in small children and infants. The technique provides a direct evaluation of liver elasticity using an impulse emitted through the skin. The propagation velocity of this impulse is proportional to the stiffness and thus to the amount of connective tissue in the liver. This stiffness is expressed in kilopascals (kPa). There have been a considerable number of studies on the use of TE in both adults and children (6–8), and the normal values for TE in children were defined by Engelmann et al. (9).

RTE is another US device for directly displaying tissue elasticity while obtaining a B-mode US before and under light compression. The changes in strain distribution in RTE are calculated by an algorithm called the "extended combined autocorrelation method," and these changes are displayed as a colored histogram. Mean value of liver elasticity is expressed in arbitrary units (a.u.). There have been numerous studies of RTE in adults (10, 11) with specific liver diseases, but the normative values with this method have not been determined in children yet.

ARFI is a further developed US method for measuring liver elasticity, using a special software package (virtual touch quantification, Siemens Healthcare), yielding a measurement in meters per second (m/s). There have been several studies that have used ARFI in children to assess liver diseases (12), and the control values for ARFI in children were recently published (13).

SWE is a novel elastography method for measuring liver elasticity in kPa with the Aixplorer ultrasound system. It displays a color-coded image superimposed on a B-mode image in real time, like RTE, using SonicTouch™ technology (14).

These methods, which share the aim of detecting liver fibrosis, are not directly comparable because they rely on different technical measurement methods and different units for their results (kPa in TE, m/s in ARFI, a.u. in RTE, kPa in SWE). This incompatibility makes the follow-up

of patients by different institutions more difficult. Not every institution can be expected to have all these methods available. Additionally, although there have been studies of specific liver diseases in pediatric patients, e.g., autosomal recessive polycystic kidney disease in TE or postchemotherapeutic changes in liver disease in pediatric oncology patients with ARFI (15, 16), a controlled histological study with elastography and histological grading has not been undertaken in pediatric patients yet. The results of these different elastography techniques, offered by different manufacturers, have not been clearly defined yet according to different stages of liver fibrosis in children or on the basis of which diseases would truly benefit from elastography. These techniques must still be analyzed in clinical settings relative to individual experiences in single centers. Therefore, in the future, controlled histological studies will be undertaken to analyze the comparability of different elastography techniques in children.

The present study aimed to make a statement about the feasibility of RTE using a phantom model and compare RTE and TE in a sample of patients with various liver diseases.

Materials and methods

RTE was performed with the Preirus™ (Hitachi) device and a 7–3 MHz linear transducer (L52). Compared to the older devices produced by Hitachi, RTE pictures have slightly better resolution with Preirus. Due to the lower frequency compared to the older Hitachi ultrasound probes, L52 allows for measurements even in patients with greater distances from the surface of the skin to the liver (e.g., in obesity and ascites). The RTE software is based on the extended combined autocorrelation method (17). The relative elasticity of liver tissue is calculated according to the strain distribution under light compression. Softer tissue can be compressed more easily than stiffer tissue; thus, the amount of displacement of the reflected ultrasound echoes is smaller in stiffer tissue. RTE displays color-coded RTE images and B-mode images simultaneously in real time (Fig. 1). On the RTE image on the left in Fig. 1, the stiffer areas are represented in blue, whereas the softer areas are represented in green and red. The color-coded RTE images are produced in RTE using the pulsing of the aorta to present tissue distortion. Every RTE examination should last at least five seconds. Thus, the RTE picture is produced as the mean of the RTE pictures from more than three heartbeats. There is a sinus curve beneath the RTE image, which shows the accuracy of the measurements (Fig. 2). After a region of interest (ROI) is chosen from the color-coded area, graded from blue to red with a 225×225 pixel matrix (length×breadth, 2.7×2.7 cm), a histogram of strain elasticity values of the matrix, in relative values from 0 to 255, is calculated in the system. A scale is produced from blue to red. The RTE software (TE 5 Elastoboard; Hitachi) generates a histogram describing the mean value of tissue elasticity (MEAN) and 10 other additional statistical values, to describe the statistical distribution of elasticity values, including AREA as the main parameter for defining the characteristics of the blue (stiffer) areas in the ROI. AREA represents the percentage proportion of blue (stiffer) areas within the ROI.

To edit these parameters and obtain a single result, several authors have developed different scoring systems (10, 18). None of these scoring systems have been validated in different pathologies or in childhood diseases or have been standardized (19). The newer elasticity score developed by Wang et al. (20) has also not been validated yet. The aim of this study was not fibrosis gradation. It was to determine the accuracy of RTE in a phantom model and to determine the correlations with TE. Additionally,

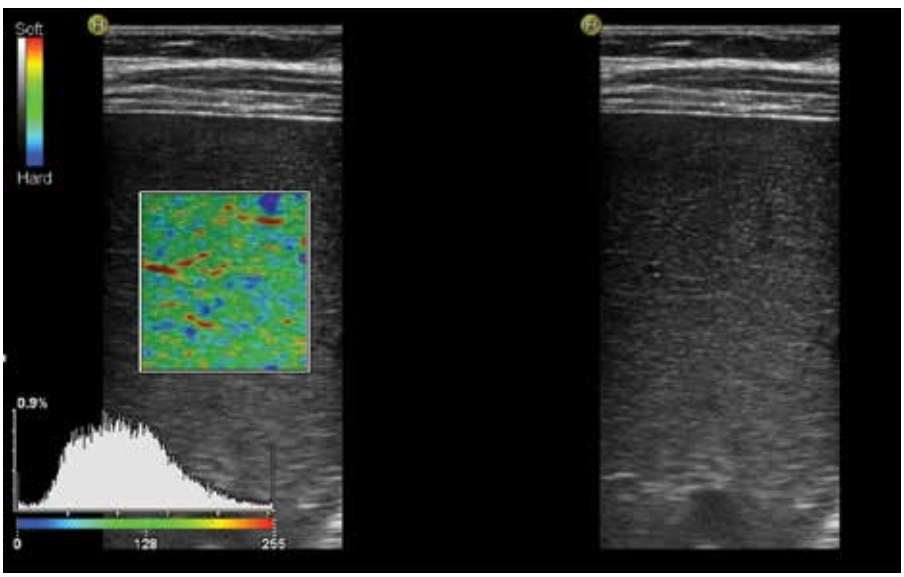

Figure 1. Stiffness is shown on a real-time tissue elastography (RTE) image on the left, according to stiffness levels in colors (red and green, soft tissue; blue, stiffer tissue). On the right side, the B-mode image appears for orientation to determine the most suitable location for a region of interest on the RTE image. A histogram of strain elasticity values of the matrix, in relative values from 0 to 255, is calculated in the system.

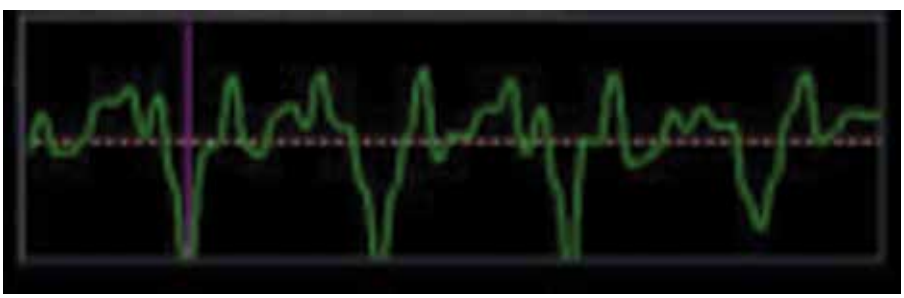

Figure 2. Sinus curve beneath the real-time tissue elastography image to show the reproducibility of the image, according to the heartbeat.

the previous study of Morikawa et al. (11) speculated that MEAN and AREA might directly represent liver elasticity. Therefore, instead of calculating a complex index, we focused on MEAN and AREA, which are recommended as important parameters by the manufacturer.

MEAN represents the mean value of tissue elasticity in a range of 0–255 a.u., which are not standard units but relative values for measuring the proportion of a certain quantity according to a reference measurement. There is a negative correlation between MEAN and stiffness. MEAN decreases, and AREA increases with increasing stiffness.

TE determines liver elasticity with an ultrasound probe by measuring the velocity of a mechanical impulse to the liver tissue. The stiffness (E) is measured in kPa, depending on the density (P) and the velocity of the shear wave of this impulse (Vs^2), using the following formula: $E=3pVs^2$ (21).

TE produces a mechanical impulse of 50 Hz lasting 20 ms. This impulse is delivered from the probe to the skin, and it continues into the depths of the skin. The elastic shear wave is measured by an US probe. During this measurement, the probe focuses on a certain defined distance from the transducer to prevent the influence of adipose tissue. There are two types of probes: an S-probe (frequency, 5 MHz; probe diameter, 5 mm) and an M-probe (frequency, 3.5 MHz; probe diameter, 7 mm). The manufacturer recommends that the measurements be performed with the M-probe on participants with a thoracic circumference greater than 75 cm. Participants with a thoracic circumference less than 75 cm should be examined with the S-probe. The S-probe has two different modes: S1 and S2. The S1 mode of the S-probe allows for measurements of small children or babies with a thoracic circumference less than 45 cm, whereas the S2 mode is suitable for measurements of participants with a thoracic circumference of 45–75 cm. The measurement depth differs with the other probes and modes: M-probe, 2.5–6.5 cm; S-probe S1 mode, 1.5–4 cm; and S-probe S2-mode, 2–5 cm.

RTE was performed on the liver tissue-mimicking Ultrasound Elasticity QA Phantom Model 049 (Computerized Imaging Reference Systems Company Inc., Norfolk, Virginia, USA) (Fig. 3). The phantom consisted of a water-based gel (Zerdine®) with tissue-equivalent ultrasound properties (sound speed, 1545±6 m/s; attenuation coefficient, 0.50±0.05 dB/cm/MHz). In the background material with an elasticity of 29.4±8% kPa, at 21°C), spherical lesions of two different sizes were introduced with four different elasticities (lesion type I, 7.3 kPa; type II, 18.8 kPa; type III, 45.9 kPa; type IV, 61.5 kPa). The examinations were performed at room temperature by an observer with more than one year of ultrasound experience in children under the supervision of two US examiners who had the most experience and highest educational level certified by the German Society of Ultrasound in Medicine (DEGUM level III of three experience levels).

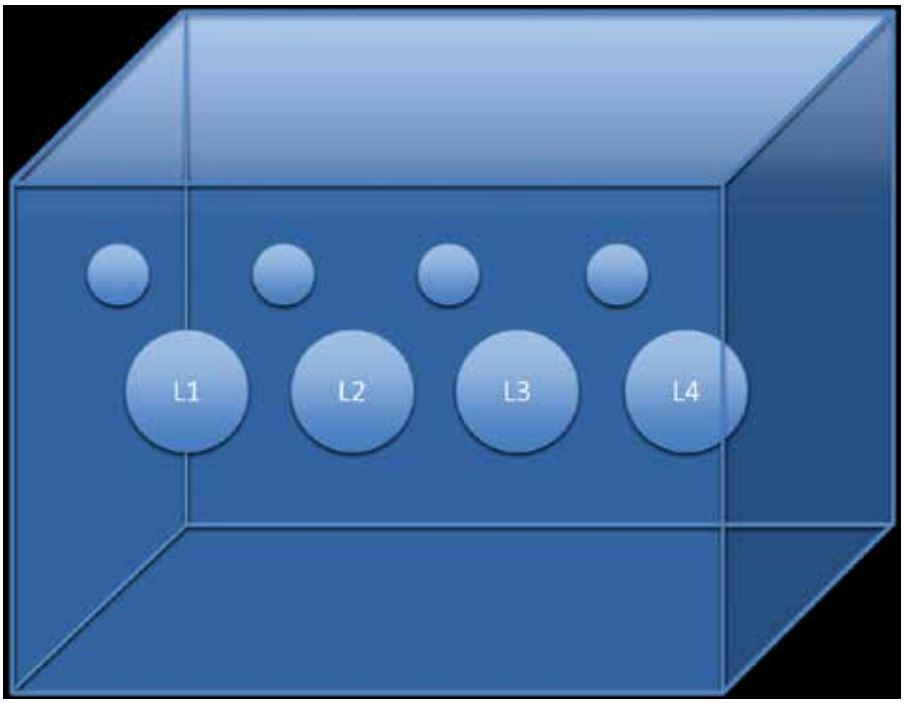

Figure 3. A three-dimensional illustration of the phantom (Elasticity QA Phantom Model 049). The phantom consisted of spherical lesions of two different sizes (diameter, 1 and 2 cm) with four different elasticities (lesion type I [L1], 7.3 kPa; type II [L2], 18.8 kPa; type III [L3], 45.9 kPa; and type IV [L4], 61.5 kPa). The real-time tissue elastography examinations were performed in the background, with larger lesions to select a region of interest as large as possible.

RTE uses the pulsing of the aorta to present tissue distortion. Because of the lack of a pulsing aorta in the phantom, the examinations were performed using minimal efficient pressure with a free-hand technique.

With the HI-RTE from HI Vision Preirus™, the stiffness of the various structures within the phantom could be visualized as a colored overlay (maximum, 2.7×2.7 cm) of the B-mode image. RTE measurements were performed at a depth of 3.5 cm in the center of the larger lesions and in the background material. To select an ROI as large as possible for the measurements in the lesions, the examinations were performed in the larger lesions (diameter, 2 cm) with two offered possibilities of lesion size. It was attempted to choose an area of 1×1 cm so the ROI would remain entirely within the lesion, without measuring the background material. Thereby the background influence on the stiffness measurements of the lesions would be minimized. First, RTE was performed in the background with an ROI of 2.7×2.7 cm. To obtain measurements approximately at the same depth in the lesions, the ROI was chosen in the background at an approximate depth of 2.2–4 cm (Fig. 4).

Ten measurements per point were obtained, and the mean values of the RTE parameters (MEAN and AREA)

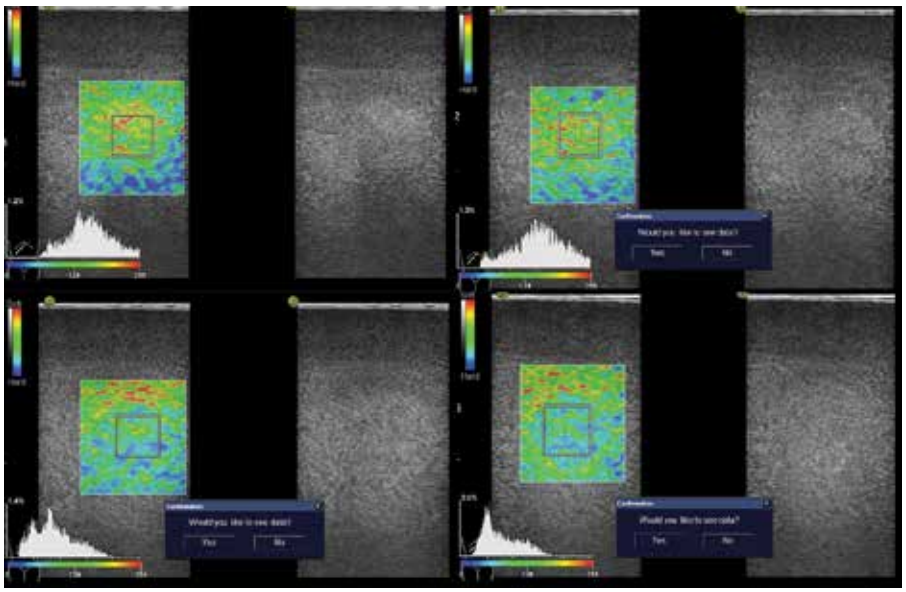

Figure 4. On the phantom, real-time tissue elastography measurements were obtained in 3.5 cm of depth in the larger lesions (diameter, 2 cm). With increasing stiffness of the lesions, the proportion of the blue area in the region of interest increased, and the histogram shifted to the left.

were calculated. Pearson's product-moment correlation test was performed to compare these mean values with phantom stiffness in kPa, which also represented the technical unit of TE. R software, version 2.10.1 (The R Foundation for Statistical Computing), was used for the statistical analyses.

The study protocol was in accordance with the Helsinki Declaration and was approved by the local ethics committee. Written consent was obtained from the participants or their parents (for children younger than 18 years old).

Between October 2010 and March 2012, a total of 147 patients younger than 20 years old (67 females, 80 males; mean age, 10.38±5.13 years), with several defined diseases with liver infestation, participated in the study. The patient group is described by laboratory findings (platelets, prothrombin time [INR], aspartate aminotransferase [SGOT], AST platelet ratio index [APRI score]), body mass index (BMI), BMI standard deviation score and clinical findings.

With both methods (RTE and TE), the measurements of the right lobe of the liver were obtained in the 7th or 8th intercostal space in the anterior axillary line, during inspiration in the supine position with the right arm elevated above the head. The participants had to lie still during the examination. The examinations were performed by two experienced observers, who were qualified and supervised by a B-mode-experienced pediatric radiologist (DEGUM level II).

On TE, participants with a thoracic circumference of less than 45 cm were examined with the S-probe in S1 mode (n=14, 9.5%), whereas the participants with a circumference between 45–75 cm were examined in S2 mode (n=53, 36%). The remainder of the participants with a thoracic circumference greater than 75 cm were examined with the M-probe (n=80, 54.5%). Each participant was examined with only one probe. Ten measurements were obtained from each participant with TE. These measurements had to be obtained within three minutes so they would not differ by more than 30% with each other (interquartile range [IQR]<30%). At least 60% of them had to be valid. The device displayed the mean value of the measurements automatically as a single result in kPa.

On RTE, three measurements were obtained from every participant, and the mean of the two parameters MEAN and AREA were calculated. RTE measurements were obtained by setting the ROI in a region without large vessels, using the simultaneous B-mode picture.

The TE measurements from 38 participants (approximately 25%) were invalid due to high IQR values, so they were excluded from the study. The included patients (n=109) had the following diseases with liver involvement: metabolic liver disease (n=25); cystic fibrosis (n=20); hepatopathy of unknown origin (n=11); autoimmune hepatitis (n=12); Wilson's disease (n=11); alpha-1 antitrypsin deficiency (n=3); autosomal recessive polycystic kidney disease (n=1); cholestatic hepatitis (n=1); Crohn disease (n=1), Epstein-Barr virus infection (n=2); extrahepatic biliary atresia (n=1); factor VII deficiency and cirrhosis (n=1); hepatitis B (n=6); hepatitis C (n=1); juvenile infantile arthritis (n=1); Byler disease (n=1); nonalcoholic steatohepatitis (n=3); kidney transplantation (n=4); medication-induced hepatitis (n=1); primary sclerosing cholangitis (n=1); and cirrhosis of unknown origin (n=1).

Our TE values from the participants were compared with the normal values of TE in children, defined by Engelmann et al. (upper limits of normal for 0–5 years: 4.4 kPa in females, 4.6 kPa in males; 6–11 years: 4.4 kPa in females, 4.6 kPa in males; 12–18 years: 4.7 kPa in females, 5.6 kPa in males) (9).

The normal RTE values for children have not been published yet. We calculated the control values in 30 healthy participants (15 females and 15 males; mean age, 10.07±5.54 years) without known liver diseases and without any of the inclusion criteria for the patient group, as described above. The MEAN and AREA values of the control group were compared with the MEAN and AREA values of the study population with various liver diseases according to the Mann-Whitney U test. The results for TE in kPa were compared with MEAN in a.u. and AREA in the same patients, and Pearson's product-moment correlation coefficients were calculated to determine the correlations.

Results

RTE in the phantom model and comparison of the parameters with phantom stiffness

By choosing ROIs in the background and in lesions (L) 1–4, following means for MEAN and AREA were calculated respectively, from the 10 measurements:

114.12±1.59 and 12.50±1.67 for background; 162.51±5.14 and 0.82±1.09 for L1; 148.83±7.19 and 1.45±1.13 for L2; 85.37±4.71 and 28.92±5.72 for L3; 76.71±6.82 and 38.26±4.39 for L4.

The RTE parameters showed strong correlation in the phantom model with the phantom stiffness specified in kPa (MEAN/kPa, r=-0.973, P = 0.005, 95% confidence interval [CI]: -0.998, -0.641; AREA/kPa, r=0.981, P = 0.003, 95% CI: 0.739, 0.999; Figs. 5, 6). There was a strong inverse correlation between phantom stiffness and MEAN; one increased while the other decreased. In the same direction, there was a strong relationship between phantom stiffness and AREA: both increased and decreased in the same direction.

Comparison of RTE and TE in the patient group

The characteristics of the included participants are shown in Table 1. The measurements for TE ranged from 2.6 to 69.1 kPa. The upper values were found in patients with metabolic liver diseases (mainly type I glycogenesis), cystic fibrosis and liver cirrhosis. Despite known diseases with liver involvement, the TE results of 42 of the 109 included patients (38.5%) were with the normal ranges, according to the normal values for children provided by Engelmann.

In 40 of 67 patients with increased TE values, an increase in liver enzymes was observed (59%). All 40 of these participants showed increased SGOT values and APRI scores. Only seven of 67 participants had pathological INR values (10%), and six participants had high platelet counts (9%).

Similar with TE, the patients with metabolic liver diseases (mainly type I glycogenesis), CF and cirrhosis showed the most significant changes in RTE. The median of MEAN in the patient group was 103 a.u., and the median of AREA was 28. The median of MEAN in our small control group was 109 a.u., and the median of AREA was 20 (Table 2).

The MEAN and AREA values showed significant differences between the study population and the small control group (MEAN, P = 5.32 e-7 at 5% significance level; AREA, P = 1.62 e-6 at 5% significance level) (Figs. 7, 8).

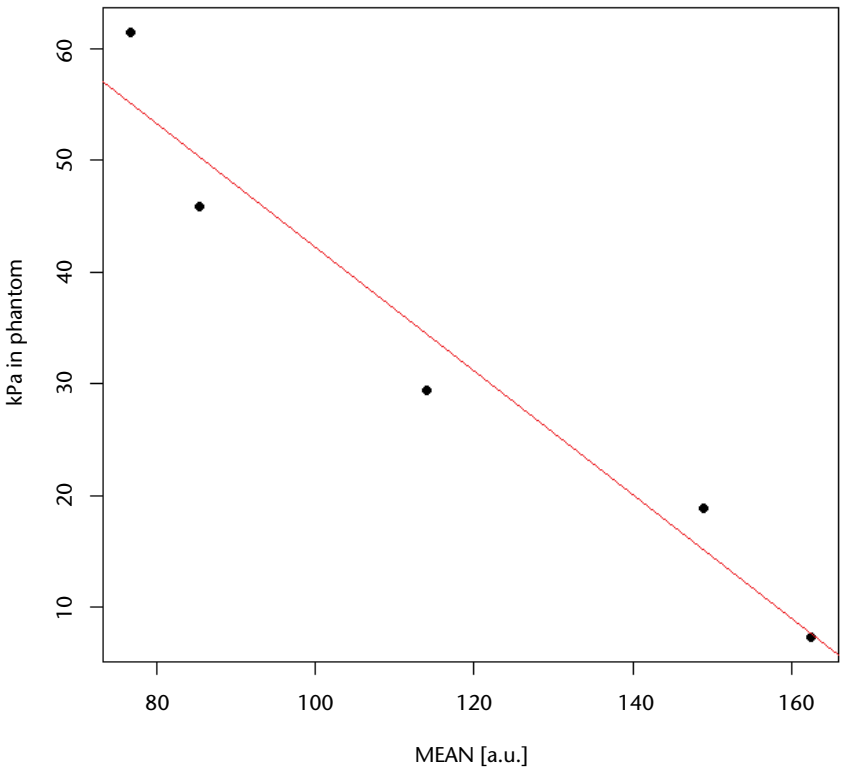

Figure 5. MEAN showed a strong correlation in the phantom model with phantom stiffness, specified in kPa (MEAN/kPa: r=-0.973, P = 0.005, 95% CI=-0.998, -0.641). MEAN, mean value of tissue elasticity in real-time tissue elastography.

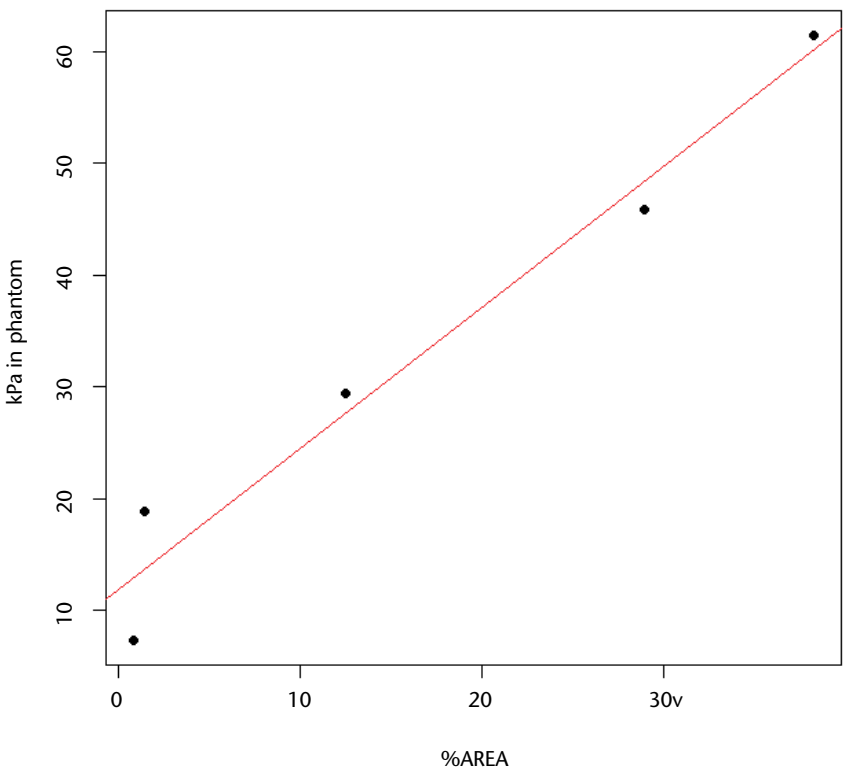

Figure 6. AREA showed a strong correlation in the phantom model with phantom stiffness, specified in kPa (AREA/kPa: r=0.981, P = 0.003, 95% CI=0.739, 0.999). AREA, real-time tissue elastography parameter to express the percentage proportion of blue (stiffer) areas within the region of interest.

Table 1. Characteristics of the study patients at the time of the real-time tissue elastography and transient elastography examinations

Characteristics	Patients (n=109)
Gender (female/male)	45/64
Age (years)	11.21 (0–20)
BMI (kg/m^2)	17.48 (11.65–34.90)
BMI-SDS	-0.015 (-4.27–-2.77)
Thrombocytes (/nL)	302 000 (149 000–869 000)
Prothrombin time (INR)	1.03 (0.90–1.40)
SGOT (U/L)	41 (13–1625)
APRI-score	1.06±2.66 (0.06–21.68)
Transient elastography (kPa)	5.9 (2.6–69.1)
MEAN (a.u.)	109 (69–119)
AREA	28 (10–60)

APRI-score, aspartate aminotransferase to platelet ratio index; AREA, percentage proportion of blue (stiffer) areas within the region of interest in real-time tissue elastography; BMI, body mass index; BMI-SDS, body mass index standard deviation score; INR, international normalized ratio; MEAN, mean value of tissue elasticity in-time tissue elastography; SGOT, aspartate aminotransferase.
Data are given as median (range).

Table 2. Distribution of MEAN values in the control group (n=30) and patient group (n=109)

MEAN	Minimum	First quarter	Median	Mean	Third quarter	Maximum
Control group	102	107	109	109	111	114
Patient group	69	96	103	101	108	119

MEAN, mean value of tissue elasticity in real-time tissue elastography.

The correlations of both methods, RTE and TE, were similar in direction but were much weaker in the patient group (MEAN/kPa, r=-0.226, P = 0.017, 95% CI=-0.397, -0.040; AREA/kPa, r=0.238, P = 0.012, 95% CI=0.052, 0.408, Figs. 9, 10).

Discussion

Several noninvasive methods have been developed lately to replace the liver biopsy, which is the gold standard for determining liver elasticity. Alternative ultrasonographic methods to detect liver fibrosis include TE, RTE, ARFI, and SWE.

These methods are not directly comparable with each other because they are based on different technical units of measurement. This incompatibility of the results complicates the follow-up of patients by different institutions. Thus, in this study, we aimed to examine the conversion of the results from these different methods, to facilitate the control of patients and to assess the feasibility of RTE in a phantom model with different stiffness levels in kPa, by performing multiple measurements.

TE belongs, like ARFI and SWE, to the dynamic elastography methods for measuring liver elasticity. In contrast, RTE is a static elastography method (22). This was the first study comparing RTE and TE in pediatric patients with clinically defined diseases.

TE measurements are not practicable in phantom models because the localization of the lesions requires B-mode US. It is impossible to obtain an exact measurement of the lesions in the phantom with TE without the effect of the phantom background. TE is rather suitable for detecting diffuse liver changes but not single lesions. However, the stiffness of the phantom lesions is predetermined by the phantom manufacturer.

With RTE, phantom lesions were easily detected on B-mode images, and ROIs were easily localized on lesions. The ROI had a quadrangular shape, which was laid over the lesions, equivalent to the procedure in patient examinations. Measurements were obtained in the larger lesions of 2 cm diameter to select an ROI as large as possible. The ROIs remained in the lesions to prevent the influence of the background. The 10 measurements of one lesion showed a small range of values in RTE, indicating the reproducibility of the measurement results. Higher values in kPa of the lesions were correlated with lower values for MEAN and higher values for AREA. The measurements in the phantom model represented the measurements of a defined distance of the reference nodule, using a free-hand technique *in vitro*. Havre et al. (23) measured the strain ratio (quotient of mean strain in reference surrounding an inclusion and mean strain inclusion), and they demonstrated that changing the size of the lesion (reference area), while keeping the center depth the same, did not influence the mean strain ratio levels significantly for *in vitro* phantom model measurements. A change of position of the reference area to a deeper position influenced the strain ratio measurements using RTE (23). Lesion

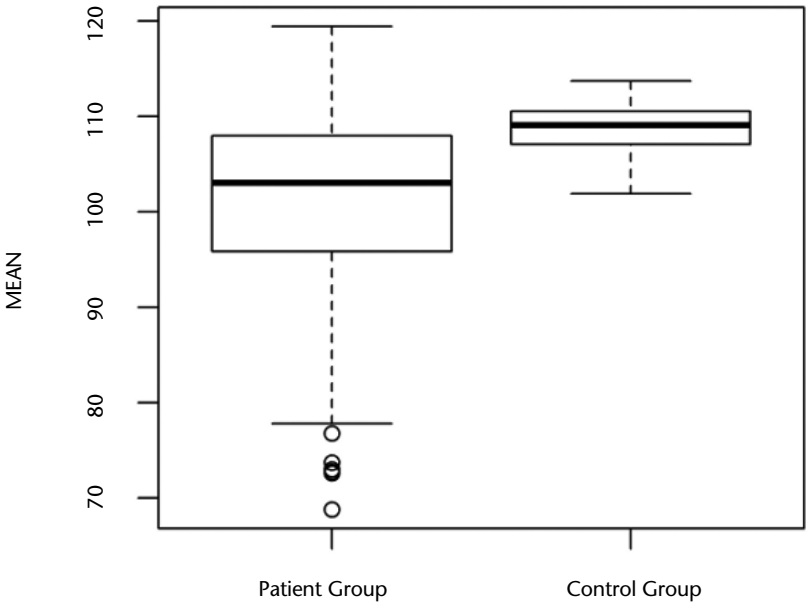

Figure 7. Comparison of the RTE parameter MEAN between the patient and control groups. MEAN, mean value of tissue elasticity in real-time tissue elastography.

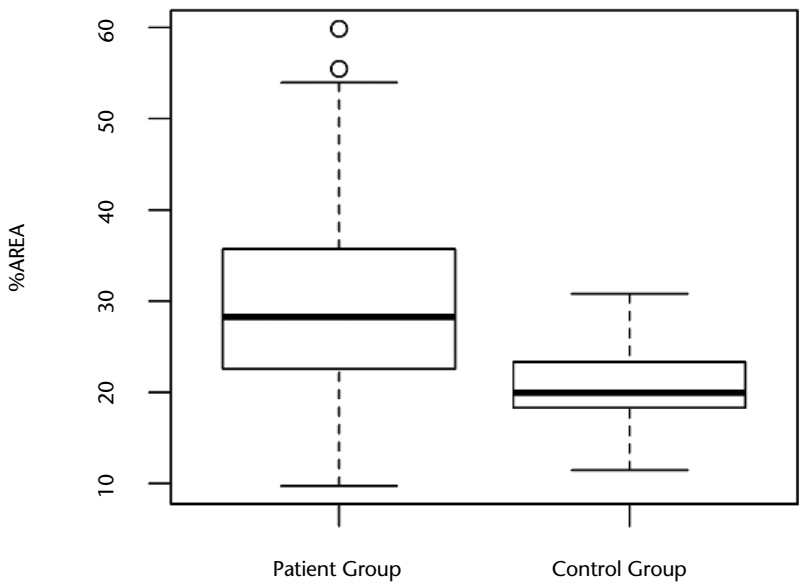

Figure 8. Comparison of the RTE parameter AREA between the patient and control groups. AREA, percentage proportion of blue (stiffer) areas within the region of interest in real-time tissue elastography.

position in our study was defined by the phantom model.

The correlations of the RTE results and the phantom stiffness levels, specified in the unit of TE (kPa), were satisfying.

Our next goal was to compare the RTE and TE methods in patients with defined liver diseases or with diseases with liver involvement.

Since the introduction of TE into daily practice in adult hepatology (5), it has continued to gain importance in pediatric patients as well. Liver stiffness measures between 2.5 kPa and 75 kPa. There have been several studies in adults to define the normal values of TE (24–26). Engelmann et al. (9) defined normal values for the pediatric age group. The upper limit of normal was dependent on the child's age and sex. In our patients, 61.5% demonstrated higher values than the upper limit of normal. Lesion 1 in the phantom model was slightly higher than the upper limit of normal values; background and lesions 2–4 represent high kPa values, expressing severe fibrosis or liver cirrhosis in adult patients (11, 24–26). However, the gradation of elastography methods in children has been missing in the literature, so the lower or higher values in TE should be interpreted with great caution in pediatric patients. As reported by Friedrich-Rust et al. (27), most elastography studies have previously been performed with transient elastography, and future studies will demonstrate whether other elastography methods that are integrated into routine ultrasound devices have similar prognostic significance in chronic liver diseases. The limitations of TE have been described in early studies, and they include ascites, elevated BMI, and intra-abdominal and central venous pressure (28–31).

In the previous study of Morikawa et al. (11), healthy adult participants and patients with hepatitis C were examined. The histological fibrosis grade was correlated with RTE parameters. Approximately 75% of the healthy participants without any liver changes or with decent grades of liver fibrosis (F1) had MEAN values greater than 100. Our pediatric control values (median of MEAN, 109) were slightly greater than the values of Morikawa et al. (11). Comparing these control values from healthy children with those from patients with liver diseases, we observed lower values for MEAN and higher values for AREA in the patient group, but with a great area of overlap with values greater than 100 a.u. for MEAN and less than 30% for AREA. Nevertheless, the difference between the two groups was statistically significant. It also should be noted that the control values for RTE cannot be interpreted as normative values because of the small number of participants in this study.

The correlations of both methods in the participants with several liver dis-

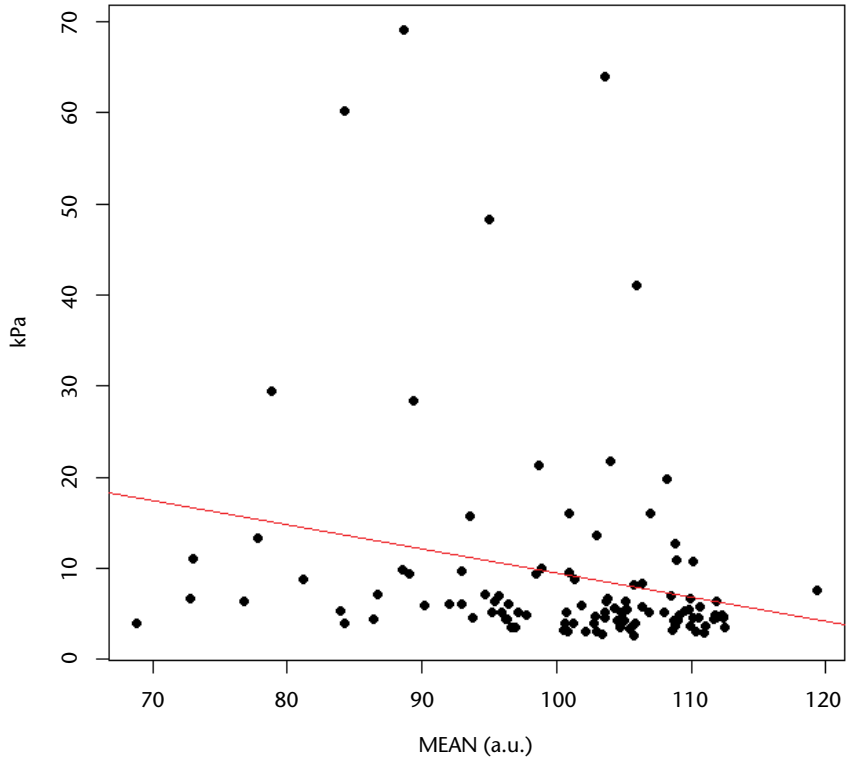

Figure 9. MEAN and transient elastography showed a weak correlation in the patients (MEAN/kPa: r=-0.226, *P* = 0.017, 95% CI=-0.397, -0.040). MEAN, mean value of tissue elasticity in real-time tissue elastography.

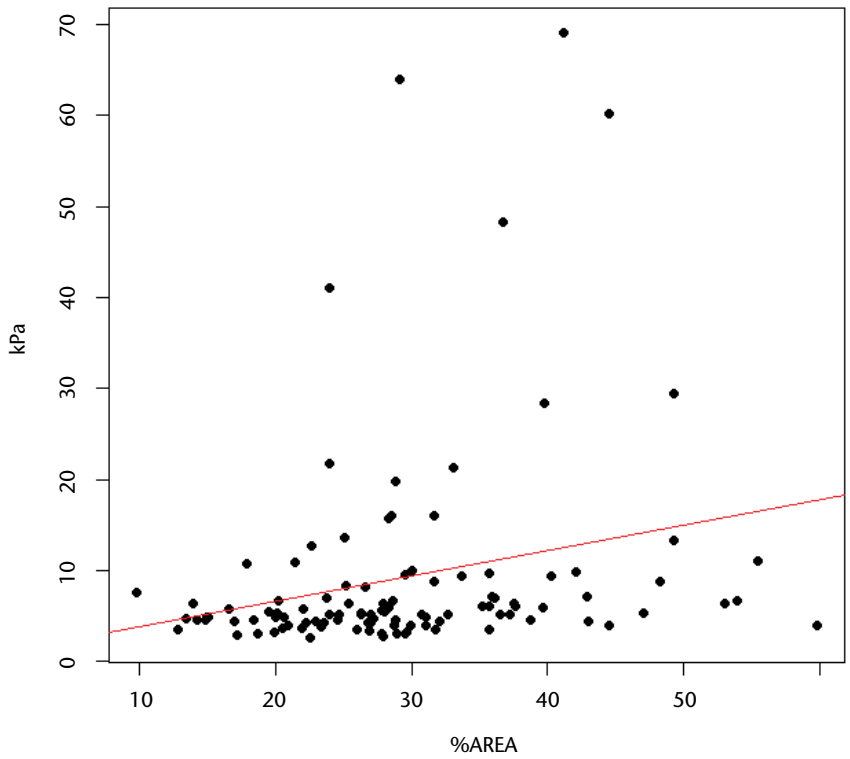

Figure 10. AREA and transient elastography showed a weak correlation in the patients (AREA/kPa: r=0.238, *P* = 0.012, 95% CI=0.052, 0.408). AREA, percentage proportion of blue (stiffer) areas within the region of interest in real-time tissue elastography.

eases were not as satisfying as the correlations between RTE and phantom stiffness. This weak correlation of both methods *in vivo* showed that they were correlated with each other, but not as strongly as they should have been to offer satisfying comparability. There was a tendency toward higher values in TE, representing lower values for MEAN in RTE and higher values for AREA.

In our opinion, there are several reasons for these differences, indicating the limitations of this study. With regard to the patient group, various factors should be considered, such as the compliance of the patients. First, strict compliance cannot always be achieved, especially with small children younger than five years old (9). In addition, the depth of breathing can vary in patients. Another difficulty is that the changing or extreme compression of the observer can influence the color code images and thus the subsequent statistical parameters on RTE (18). Although the examinations were performed by two experienced observers, and the latest available probe was used for the RTE measurements to prevent this difficulty, there was still an irrepressible error rate. An important limitation of the phantom study was the free-hand technique used, rather than using a pressure-defined mechanical setting. To minimize the effect of manual pressure, the manual pressure applied to the phantom was minimal, only sufficient to achieve a colored elastography picture.

When manual pressure, using the free-hand technique in the phantom model, generated the elastogram, tissue movement was generated by the pulse, which generated the elastogram in patients, causing great difference between the two presented correlation studies.

Other differences between the measurements in the phantom model and in the patients were the measurement depth, the size of the ROI and the number of investigators. In the phantom study, the measurements were obtained at 3.5 cm of depth in the lesions and at approximately 2.2–4 cm of depth in the background. However, in the patients, the measurements were

obtained at a depth 1 cm below the liver capsule, as instructed by the manufacturer. The size of the ROI on the 4 phantom lesions was 1x1 cm, whereas it was 2.7×2.7 cm in the patients and in the background of the phantom. The TE measurements were obtained with an S-probe (S1- and S2-mode) or M-probe depending on the patients' thoracic diameters. The depth of measurement with the S-probe was 1.5–4 cm in S1-mode and 2–5 cm in S2-mode. The M-probe measured to a depth of 2.5–6.5 cm, i.e., different from the ROI measurement depth in patients (1–3.8 cm). In addition, the depth of the subcutaneous adipose tissue differed in each patient, whereas the depth in the phantom was constant. In the phantom study, the measurements were obtained by the same investigator; however, in the patient group, they were obtained by two experienced, but different, investigators. Additionally, the vessels have high elasticity and can affect the measurements. Therefore, in this study, we attempted to select possibly avascular regions by detecting the branches of the portal veins with simultaneous B-mode imaging. However, it was not always possible to avoid the small vessels during the measurements in the patient group because of the larger size of the ROI. Additionally, exact correlation of a synthetic polymer in a stiff box cannot be expected with the biological tissues encountered in clinical examinations.

The aim of this study was not to correlate single values from TE or RTE with the stage of fibrosis in different diseases but was to determine the correlation of the values with TE and RTE. However, it seemed to be a limitation of this study that the study population was not a homogenous group of patients with the same diseases. Additionally, the participants with the same liver diseases were not in the same stages of liver structure changes, and the cases were not histologically controlled.

Another important limitation of our study was that we could not study the inter- or intraobserver variability of RTE, because most of the participants in the pediatric study group could not tolerate longer examination times or repetitive measurements by two observers successively with the two elasticity methods.

In conclusion, based on our findings, we do not recommend transferring the results produced with TE directly to RTE or vice versa in pediatric patients. To come to a more accurate decision about the grading of diffuse liver pathology in pediatric patients using different elastography methods, further studies are necessary with histologically defined liver structure changes from liver biopsy. In the future, it will be important to calculate the values from different elastography methods in different stages of liver fibrosis in specific pediatric liver diseases.

Acknowledgements

This study was funded by Dietmar Hopp Foundation.

Conflict of interest disclosure

The authors declared no conflicts of interest.

References

1. Abdi W, Millan JC, Mezey E. Sampling variability on percutaneous liver biopsy. Arch Intern Med 1979; 139:667–669. [CrossRef]
2. Castéra L, Nègre I, Samii K, Buffet C. Pain experienced during percutaneous liver biopsy. Hepatology 1999; 30:1529–1530. [CrossRef]
3. Piccinino F, Sagnelli E, Pasquale G, Giusti G. Complications following percutaneous liver biopsy. A multicentre retrospective study on 68,276 biopsies. J Hepatol 1986; 2:165–173. [CrossRef]
4. Maharaj B, Maharaj RJ, Leary WP, et al. Sampling variability and its influence on the diagnostic yield of percutaneous needle biopsy of the liver. Lancet 1986; 1:523–525. [CrossRef]
5. Sandrin L, Fourquet B, Hasquenoph JM, et al. Transient elastography: a new noninvasive method for assessment of hepatic fibrosis. Ultrasound Med Biol 2003; 29:1705–1713. [CrossRef]
6. Castéra L, Vergniol J, Foucher J, et al. Prospective comparison of transient elastography, Fibrotest, APRI, and liver biopsy for the assessment of fibrosis in chronic hepatitis C. Gastroenterology 2005; 128:343–350. [CrossRef]
7. Castéra L, Forns X, Alberti A. Non-invasive evaluation of liver fibrosis using transient elastography. J Hepatol 2008; 48:835–847. [CrossRef]
8. de Ledinghen V, Douvin C, Kettaneh A, et al. Diagnosis of hepatic fibrosis and cirrhosis by transient elastography in HIV/hepatitis C virus coinfected patients. J Acquir Immune Defic Syndr 2006; 41:175–179. [CrossRef]
9. Engelmann G, Gebhardt C, Wenning D, et al. Feasibility study and control values of transient elastography in healthy children. Eur J Pediatr 2012; 171:353–360. [CrossRef]
10. Tatsumi C, Kudo M, Ueshima K, et al. Non-invasive evaluation of hepatic fibrosis for type C chronic hepatitis. Intervirology 2010; 53:76–81. [CrossRef]
11. Morikawa H, Fukuda K, Kobayashi S, et al. Real-time tissue elastography as a tool for the noninvasive assessment of liver stiffness in patients with chronic hepatitis C. J Gastroenterol 2011; 46:350–358. [CrossRef]
12. Noruegas MJ, Matos H, Gonçalves I, Cipriano MA, Sanches C. Acoustic radiation force impulse imaging in the assessment of liver fibrosis in children. Pediatr Radiol 2012; 42:201–204. [CrossRef]
13. Eiler J, Kleinhildermann U, Albers D, et al. Standard value of ultrasound elastography using acoustic radiation force impulse imaging (ARFI) in healthy liver tissue of children and adolescents. Ultraschall in Med 2012; 33:474–479. [CrossRef]
14. Sporea I, Sirli RL. Hepatic elastography for the assessment of liver fibrosis-present and future. Ultraschall in Med 2012; 33:550–558. [CrossRef]
15. Kummer S, Sagir A, Pandey S, et al. Liver fibrosis in recessive multicystic kidney diseases: transient elastography for early detection. Pediatr Nephrol 2011; 26:725–731. [CrossRef]
16. Mârginean CO, Baghiu MD, Branzaniuc K, et al. The role of real-time elastography in the evaluation of post chemotherapy hepatotoxicity in children with cancer. Rev Med Chir Soc Med Nat Iasi 2011; 115:70–77.
17. Yamakawa M, Shiina T. Strain estimation using the extended combined autocorrelation method. Jpn J Appl Phys 2001; 40:3872–3876. [CrossRef]
18. Friedrich-Rust M, Ong MF, Herrmann E, et al. Real-time elastography for noninvasive assessment of liver fibrosis in chronic viral hepatitis. AJR Am J Roentgenol 2007; 188:758–764. [CrossRef]
19. Friedrich-Rust M, Schwarz A, Ong M, et al. Real-time tissue elastography versus FibroScan for noninvasive assessment of liver fibrosis in chronic liver disease. Ultraschall in Med 2009; 30:478–484. [CrossRef]
20. Wang J, Guo L, Shi X, Pan W, Bai Y, Ai H. Real-time elastography with a novel quantitative technology for assessment of liver fibrosis in chronic hepatitis B. Eur J Radiol 2012; 81:e31–36. [CrossRef]
21. Royer D, Dieulesaint E. Elastic waves in solids. New York: Springer Verlag, 2000. [CrossRef]
22. Morikawa H. Real-time tissue elastography and transient elastography for evaluation of hepatic fibrosis. In: Tagaya N, ed. Liver biopsy--indications, procedures, results. Croatia: Rijeka, 2012; 281–292. [CrossRef]

23. Havre RF, Waage JR, Gilja OH, Odegaard S, Nesje LB. Real-time elastography: strain ratio measurements are influenced by the position of the reference area. Ultraschall Med 2011; 33:559–568.
24. Kim SU, Choi GH, Han WK, et al. What are "true normal" liver stiffness values using FibroScan?: a prospective study in healthy living liver and kidney donors in South Korea. Liver Int 2010; 30:268–274. [CrossRef]
25. Das K, Sarkar R, Ahmed SM, et al. "Normal" liver stiffness measure (LSM) values are higher in both lean and obese individuals: a population-based study from a developing country. Hepatology 2012; 55:584–593. [CrossRef]
26. Kumar M, Sharma P, Garg H, Kumar R, Bhatia V, Sarin SK. Transient elastographic evaluation in adult subjects without overt liver disease: influence of alanine aminotransferase levels. J Gastroenterol Hepatol 2011; 26:1318–1325. [CrossRef]
27. Friedrich-Rust M, Vermehren J. Non-invasive methods for the evaluation of liver fibrosis in clinical practice. Z Gastroenterol 2013; 51:43–54.
28. Millonig G, Reimann FM, Friedrich S, et al. Extrahepatic cholestasis increasis liver stiffness (Fibroscan) irrespective of fibrosis. Hepatology 2008; 48: 1718–1723. [CrossRef]
29. Millonig G, Friedrich S, Adolf S, et al. Liver stiffness is directly influenced by central venous pressure. J Hepatol 2010; 52:206–210. [CrossRef]
30. Calvaruso V, Camma C, Di Marco V, et al. Fibrosis staging in chronic hepatitis C: analysis of discordance between transient elastography and liver biopsy. J Viral Hepat 2010; 17:469–474.
31. Castéra L, Foucher J, Bernard P, et al. Pitfalls of liver stiffness measurement: a 5-year prospective study of 13,369 examinations. Hepatology 2010; 51:828–835.